Solar Radiation Management Impacts on Agriculture in China: A Case Study in the Geoengineering Model Intercomparison Project (GeoMIP)

Lili Xia,[1] Alan Robock,[1] Jason Cole,[2] Charles L. Curry,[3] Duoying Ji,[4] Andy Jones,[5] Ben Kravitz,[6] John C. Moore,[4] Helene Muri,[7] Ulrike Niemeier,[8] Balwinder Singh,[6] Simone Tilmes,[9] Shingo Watanabe,[10] and Jin-Ho Yoon[6]

[1]Department of Environmental Sciences, Rutgers University, New Brunswick, NJ, USA
[2]Canadian Centre for Climate Modeling and Analysis, Environment Canada, Toronto, ON, Canada
[3]School of Earth and Ocean Sciences, University of Victoria, Victoria, Canada
[4]State Key laboratory of Earth Surface Processes and Resource Ecology, College of Global Change and Earth Science, Beijing Normal University, Beijing, China
[5]Met Office Hadley Center, Exeter, UK
[6]Atmospheric Sciences and Global Change Division, Pacific Northwest National Laboratory, Richland, WA, USA
[7]Department of Geosciences, Meteorology and Oceanography, University of Oslo, Oslo, Norway
[8]Max Planck Institute for Meteorology, Hamburg, Germany
[9]National Center for Atmospheric Research, Atmospheric Chemistry Division, Boulder, CO, USA
[10]Japan Agency for Marine-Earth Science and Technology, Yokohama, Japan

Submission to *Journal of Geophysical Research – Atmospheres*
GeoMIP special issue

July, 2013

Revised, January, 2014

Revised again, April 2014

Revised again, June 2014

Corresponding author:
Lili Xia
Department of Environmental Sciences
Rutgers University
14 College Farm Road
New Brunswick, NJ 08901
Email: lxia@envsci.rutgers.edu

This article has been accepted for publication and undergone full peer review but has not been through the copyediting, typesetting, pagination and proofreading process which may lead to differences between this version and the Version of Record. Please cite this article as doi: 10.1002/2013JD020630

Abstract

Geoengineering via solar radiation management could affect agricultural productivity due to changes in temperature, precipitation, and solar radiation. To study rice and maize production changes in China, we used results from 10 climate models participating in the Geoengineering Model Intercomparison Project (GeoMIP) G2 scenario to force the Decision Support System for Agrotechnology Transfer (DSSAT) crop model. G2 prescribes an insolation reduction to balance a 1% per year increase in CO_2 concentration (1pctCO2) for 50 years. We first evaluated the DSSAT model using 30 years (1978-2007) of daily observed weather records and agriculture practices for 25 major agriculture provinces in China, and compared the results to observations of yield. We then created three sets of climate forcing for 42 locations in China for DSSAT from each climate model experiment: (1) 1pctCO2, (2) G2, and (3) G2 with constant CO_2 concentration (409 ppm), and compared the resulting agricultural responses. In the DSSAT simulations: (1) Without changing management practices, the combined effect of simulated climate changes due to geoengineering and CO_2 fertilization during the last 15 years of solar reduction would change rice production in China by -3.0±4.0 Mt (2.4±4.0%) as compared with 1pctCO2 and increase Chinese maize production by 18.1±6.0 Mt (13.9±5.9%); (2) The termination of geoengineering shows negligible impacts on rice production but a 19.6 Mt (11.9%) reduction of maize production as compared to the last 15 years of geoengineering; (3) The CO_2 fertilization effect compensates for the deleterious impacts of changes in temperature, precipitation, and solar radiation due to geoengineering on rice production, increasing rice production by 8.6 Mt. The elevated CO_2 concentration enhances maize production in G2, contributing 7.7 Mt (42.4%) to the total increase. Using the DSSAT crop model, virtually all of the climate models agree on the sign of the responses, even though the spread across models is large. This suggests that solar radiation management would have little impact on rice production in China, but could increase maize production.

Keywords: GeoMIP, G2, rice production, maize production, DSSAT, geoengineering, SRM, solar radiation management

1. Introduction

Solar radiation management (SRM) has been discussed as a possible remedy for global climate warming [e.g., *Crutzen*, 2006; *Wigley*, 2006]. Although this strategy would likely reduce global temperatures [e.g., *Govindasamy and Caldeira*, 2000; *Robock et al.*, 2008; *Jones et al.*, 2010], there could be side effects that strongly influence the climate system and society [e.g., *Robock*, 2008]. One possible side effect is an increased risk to food security due to the climate changes resulting from geoengineering, especially in regions where agriculture productivity is highly determined by the summer monsoon system [e.g., *Robock et al.*, 2008]. A temperature gradient reduction between the continent and ocean in East Asia could reduce summer monsoon circulation, possibly affecting East Asian agriculture [*Robock et al.*, 2008; *Tilmes et al.*, 2013]. However, it has been difficult to determine robust effects on agriculture in this region, as *Robock et al.* [2008], *Rasch et al.* [2008], and *Jones et al.* [2010] all found different regional climate responses to geoengineering. Recently, the Geoengineering Model Intercomparison Project (GeoMIP) [*Kravitz et al.*, 2011] set up four geoengineering scenarios for climate modeling groups to better understand climate responses to SRM, providing a good opportunity for an agriculture impact study. Here we use 10 climate modeling groups' results from the G2 scenario, in which a 1% per year CO_2 increase (1pctCO2) [*Taylor et al.*, 2012], is balanced by a reduction in insolation for 50 years, followed by no insolation reduction for another 20 years, to investigate any effects of rapid cessation of SRM (also called "termination effects" [e.g., *Wigley*, 2006; *Matthews and Caldeira*, 2007; *Robock et al.*, 2008; *Jones et al*., 2013].

Agricultural productivity is expected to be sensitive to climate change. Temperature, precipitation, solar radiation, and CO_2 concentration are the important climate factors affecting agriculture. There have been many studies of how climate changes influence food production using different methods, such as field experiments [e.g., *Long et al.*, 2006],

empirical statistical models [e.g., *Lobell et al.*, 2011; *Pongratz et al.*, 2012] and dynamic crop models [e.g., *Parry et al.*, 2004].

Pongratz et al. [2012] used a temperature-precipitation-CO_2 statistical model under a geoengineered high-CO_2 world forced by simulated climate changes from two climate models, and found that global rice, maize and wheat yields increase due to CO_2 fertilization and less heat stress, and also found that there are possible regional rice yield losses in the middle latitudes of the Northern Hemisphere. Here we expand on that study by using the results from 10 climate models and a mechanistic model of crop production, focusing on China, the country with the largest rice production and the second largest maize production in the world [*FAO*, 2012]. We examine rice and maize production in China and address three questions here: (1) How would rice and maize production in China change under solar geoengineering? (2) How would rice and maize production in China change when geoengineering is abruptly ended? (3) Among temperature, precipitation, solar radiation, and CO_2 concentration, which are the dominant factors controlling regional agriculture responses?

2. Methodology

2.1. Crop Model Evaluation

We used the Decision Support System for Agrotechnology Transfer (DSSAT) model version 4.5 to simulate crop response to climate changes [*Jones et al.*, 2003; *Hoogenboom et al.*, 2012]. This dynamic biophysical crop model simulates crop growth on a per hectare basis, maintaining balances for water, carbon, and nitrogen. It requires information about the plant environment (weather, atmospheric CO_2 concentration, and soil properties), cultivar genotype, and agricultural management practices. Different factors are important at different phenological phases of each crop's growth. DSSAT has been evaluated for rice in 24 provinces (autonomous regions/municipalities) in China [*Xia and Robock*, 2013], and we

further evaluate this model for maize here using the same method. There are eight provinces using the same weather observations as in the rice evaluation, and the other 17 provinces use different weather station records (Table 1). Chinese weather data are from the China Meteorological Data Sharing Service System http://cdc.cma.gov.cn/.

Figure 1 shows maize evaluation results in major maize production provinces. We used the same procedure as *Xia and Robock* [2013]. Twenty-five locations with weather stations were selected, nearby soil profiles from the World Soil Information Database [*Batjes*, 2008, 2009] were used, and agriculture practices are from *Ministry of Agriculture of the People's Republic of China* [2009]. The upward trend of crop yield is mainly due to agriculture management, particularly increasing fertilizer usage. These seven provinces have the highest production in China, accounting for more than 60% of China's maize in 2008 [*Ministry of Agriculture of the People's Republic of China*, 2009]. The coefficient of determination, R^2, between observations and simulations in the seven major maize production provinces is 0.77 and in all 25 provinces R^2 is 0.57. Figure 1 also shows time series of maize yield in the seven provinces. In certain provinces in some years, such as 1985 and 1989 in Liaoning, maize yield is lower than simulated by our model. There could be many reasons for those differences, such as unrecorded changing maize cultivar or planting date. In general, our model is able to simulate rice and maize yield in major crop yield provinces in China well in terms of upward trend, average and standard deviation. If we sum up the crop production for all 25 provinces, the observations increase at a rate of 2.18 Mt a^{-1} for rice and 2.19 Mt a^{-1} for maize. Our simulations show rates of 2.12 Mt a^{-1} for rice and 2.42 Mt a^{-1} for maize, which indicates that the long term trend of observations and simulations are consistent.

Although the DSSAT model in this study is suggestive of what might happen in the future, its implementation has limitations. First of all, crop yield data are province-averaged. As we chose one weather site to represent the whole province, the simulated averaged crop

yield might not reflect the weather changes for the entire province. Second, the agriculture management information is insufficient. There are many agricultural practices DSSAT requires as input, but they were not recorded. For example, we do not know the detailed genetic information of the cultivars during the simulated period; irrigation data are missing; fertilizer types, the timing of applying, and usage amount are not fully recorded; planting density, depth and other agricultural practice details are missing .

In addition, since the upward trend of crop yields is mainly produced by the increasing of fertilizer usage, with a small contribution from CO_2 increases, we also show the comparison between the observed yields and yields in the control run without fertilizer and CO_2 forcing (Figure 1). The control run of the DSSAT model is defined as the crop yield driven by 30 years of weather observations plus 0.5 K with irrigation turned off and CO_2 concentration fixed. For rice, the R^2 is 0.02 and for maize, it is 0.06. In this case, compared with our evaluation results (R^2 for rice = 0.76, and R^2 for maize = 0.57), climate changes (temperature, precipitation, and solar radiation) only contribute a very small part of the explained variance of the historical record, 2.6% for rice and 10.5% for maize. However, the large variation of the control lines shows that DSSAT is sensitive to weather changes in terms of temperature, precipitation, and solar radiation (Figure 1). With fixed fertilizer and no irrigation, we expect that the simulated crop yield would not be highly correlated with the historical record, because the observed crop yields are controlled by natural weather variation and human agriculture management. In addition, we did sensitivity tests at Hainan for rice to test how DSSAT reacts to temperature, precipitation and solar radiation changes in different seasons. Sensitivity tests were driven by modified daily weather based on observations in 2007 at Hainan. Rice yield is sensitive to climate changes in spring at this location. Increasing daily maximum temperature and daily minimum temperature by 1ºC would decrease rice yield by 5%. Decreasing daily precipitation by 20% would decrease rice yield

by 5% and this crop yield reduction would be 40% if daily precipitation decreases by 40%. Solar radiation also affects rice yield. With a 20% reduction, rice yield would decrease 5%.

2.2. Downscaling of Climate Model Data for DSSAT

We derived climate forcing due to SRM from 10 climate models participating in G2 (Table 2). Their pre-industrial (piControl), 1pctCO2, and G2 runs were used. We extracted monthly maximum temperature, monthly minimum temperature, monthly precipitation, and monthly surface downwelling solar radiation for 42 locations in China; 25 locations for rice and 25 locations for maize, with 8 overlapping locations. The so-called "delta" method [*Hawkins et al.*, 2013] is used in this study to create climate input for the crop model (Figure 2). In this method, two sets of anomalies of monthly average maximum temperature, minimum temperature and solar radiation (between G2 and piControl runs and between 1pctCO2 and piControl runs) were linearly interpolated to daily values and added to the observed daily climate variables. The anomaly of monthly average precipitation was divided by the observed monthly average precipitation, and daily precipitation was changed by that fraction on each day when precipitation occurred.

There are many other ways to downscale general circulation model output for impact study, such as the delta method with changing variance, and bias correction without or with changing of variance. However, in this study, we used the simplest downscaling method, the delta method without changing of variance, since it has been shown to be a relatively robust method of temperature downscaling in terms of generating future temperature change to feed crop models [*Hawkins et al.*, 2013]. We did not consider changes of variance in the simulations. In the *Curry et al.* [2014] study of the GeoMIP G1 scenario (balancing $4\times CO_2$ by insolation reduction), which was much more extreme than the G2 one we used, there were only small changes in temperature and precipitation extremes, so we do not expect this to have a major impact on our results. If we had studied a scenario where the mean climate

changed, such as the GeoMIP G4 experiment (injection of 5 Tg SO_2 to the stratosphere each year), then perhaps the frequency of frost events or damaging high temperature events would change, but when the mean does not change as in G2, the variance does not change much. We did treat changes of maximum and minimum temperature separately, and this accounts for any changes of the diurnal cycle.

2.3. Experimental Design

Since there are three climate model experiments – piControl, 1pctCO2 and G2 – and we would like to compare agriculture productivity between the 1pctCO2 world and the G2 world, two sets of climate anomalies were calculated (Figure 3): (1) anomalies between piControl and 1pctCO2, and (2) anomalies between piControl and G2.

Because we wished to use DSSAT to analyze changes in agriculture beginning in the year 2020 (the same as the beginning of the GeoMIP G3 and G4 scenarios), we performed a scaling of our results to account for higher CO_2 concentration and temperature. According to the all the RCP scenarios, global temperature increases from the average over the reference state for which we have observations (1978-2007) and the year 2020 are approximately 0.5 K. Therefore, temperature values provided to DSSAT were the temperature anomalies discussed in the previous paragraph plus 0.5 K. As simulations show small changes of precipitation in the future climate over China (Figure 3), we did not adjust the precipitation.

In the design of GeoMIP, there are 70 years of simulations for the G2 scenario (50 years of geoengineering and 20 years of post-geoengineering). We chose 30 years for our study: the last 15 years of geoengineering (36th through the 50th year), since that period has the strongest climate signal of geoengineering, and the first 15 years of post-geoengineering (51st through the 65th year) to study the termination effect on agriculture, during a period with CO_2 concentration increasing from 585 ppm to 781 ppm (CO_2 concentration estimated by 1% increases per year starting from 409 ppm in 2020).

In this study, we tested 30 climate conditions (observations for 1978-2007) for each year of the 30-year G2 and 1pctCO2 simulations. Each year of the 30-year climate anomalies of each climate model was used to perturb each of the 30 years of observations using the delta method described above. Therefore, for each year of the 30-year G2 and 1pctCO2 simulations, there are 30 simulations of rice and maize growth in 25 locations in China. In addition, to test the CO_2 fertilization effect, we created one more set of runs with G2 climate conditions (maximum temperature, minimum temperature, precipitation and solar radiation) and a constant CO_2 concentration estimated by linear extrapolation from the Mauna Loa data (http://www.esrl.noaa.gov/gmd/ccgg/trends/) for 1993-2012 to be 409 ppm in 2020. In total, there are 900 (years) × 25 (locations) × 2 (crops) × 3 (sets of runs) × 10 (climate models) + [for the control run] 30 (years) × 25 (locations) × 2 (crops) = 1,353,000 simulations.

Although in reality, agricultural practices will change depending on climate and human decisions [*Rosenzweig and Parry*, 1994; *Pongratz et al.*, 2012], in this study, to emphasize how simulated climate changes would impact agriculture yields, we fixed cultivars and agricultural practices [*Zhang et al.*, 2004; *Yao et al.*, 2007; *Dai et al.*, 2008; *Fan et al.*, 2010] in the control, G2, and 1pctCO2 runs: rice was planted on March 25 and maize was planted on April 19 (spring maize) or May 30 (summer maize) along with 150 kg/ha fertilizer applied, and the crops were harvested at maturity in fall. During all simulations, to emphasize the influence of precipitation changes, no irrigation was applied. In the control run, the CO_2 concentration was 409 ppm.

3. Results and Discussion

3.1. Climate anomalies

Figure 3 shows the 3-month moving average of monthly climate anomalies of G2 and 1pctCO2 from 10 climate models averaged over 42 locations in China compared with pre-industrial conditions. SRM results in balancing global warming in all climate models, as was

also shown by *Jones et al.* [2013]. Compared with 1pctCO2, where the average temperature anomaly (as compared to piControl) is 1.4±0.3 K during years 36-50 (Figure 3d), solar reduction cools the 42 locations by 1.2±0.1 K (Figures 3a and 3d) due to less solar energy received in the atmosphere and at the surface (Figure 3b). This cooling achieves the goal of G2, solar radiation reduction to counteract the forcing of 1pctCO2, but does not return the surface temperature at those 42 locations to the pre-industrial level completely. Except for BNU-ESM and NorESM1-M, the other eight models bring surface temperatures down to their pre-industrial values with the temperature anomalies ranging from -0.3±0.7 K (MIROC-ESM) to 0.4±0.3 K (HadGEM2-ES) during the period of years 36-50. After the end of geoengineering, global mean temperature rises rapidly in the first three years with an annual average increase of 0.5 K, 0.3 K, and 0.5 K, respectively, which is ~10 times higher than the normal annual temperature increase in 1pctCO2. Five years after geoengineering cessation, the geoengineered conditions are still 0.5 K cooler than non-geoengineered conditions at the 42 locations, which is consistent with global average temperature changes [*Jones et al.*, 2013]. Thirteen years after the end of geoengineering, averaged temperature anomalies are back to the level of 1pctCO2 with a *p*-value of 0.14.

Jones et al. [2013] found that global average precipitation change is positive in 1pctCO2 with anomalies of ~0.05 mm/day at the end of the 50th year and negative to no change under G2, with a range of changes from -0.06 to 0.00 mm/day. The average of regional precipitation changes in China of the 10 climate models is consistent with the global average, but there are large variations in different models (Figures 3c and 3f). At the end of the 50th year of 1pctCO2, nine models show positive annual precipitation change ranging from 0.02±0.39 mm/day (NorESM1-M) to 0.42±0.21 mm/day (CanESM2), except for MIROC-ESM, with a value of -0.10±0.47 mm/day. In G2, compared to 1pctCO2 years 36-50, geoengineering reduced precipitation at 42 locations and this reduction is significant with

a p-value of 3.11×10^{-21} (Figure 3c). The precipitation difference for G2 between years 36-50 and years 51-65 is 0.1 mm/day. CCSM-CAM4 is the only model not showing this trend, with no significant precipitation increase after termination of geoengineering.

3.2. Rice production changes

Chinese rice production is defined as:

$$Chinese\ Rice\ production = \sum_{i=1}^{25} (Yield_{G2,1pctCO2})_i \times (Rice\ planting\ area_{2008})_i$$

where i is the province, and $Yield_{G2,1pctCO2}$ is rice yield driven by the climate of G2 or 1pctCO2. The average simulated rice production for the 10 models in G2 is 7.0±2.6 Mt (6.7±2.5%) less than that of the control run for the 15-year period at the end of SRM (Table 3). After the end of geoengineering, simulated rice production rises, but is still 1.8±6.7 Mt less than that of the piControl run (Figure 4a). Under the 1pctCO2 scenario, rice production varies about the control run level during all 30 years (Figure 4b). All the changes are within the natural variability of rice production (defined as one standard deviation of the 1978-2007 control run).

Climate anomalies from the 10 climate models lead to different rice production responses. Nine models show negative changes of rice production (from –12.6±8.6 Mt for MIROC-ESM to –2.1±3.8 Mt for HadGEM2-ES) during the last 15 years of G2 geoengineering (years 36-50) compared to piControl, while one model (BNU-ESM) shows very slightly positive changes (1.0±5.2 Mt) in rice production (Figure 5a). This is because the G2 simulation of BNU-ESM is only partially successful at offsetting the temperature increase in 1pctCO2 [Figure 1 of *Jones et al.*, 2013]. Compared with years 36-50, during years 51-65, all models show a slight increase of rice production ranging from 2.9 Mt (MPI-ESM-LR) to 7.6 Mt (CanESM2) (Figures 4a, 5a and 5b). MPI-ESM-LR has a rapid drop of rice production in the 51st year compared with other models. A possible reason is that in the 51st year in this model, there is a relatively cold spring that is 1.5 K cooler than the average

spring temperature compared to the other models, and a relative dry summer and fall, with precipitation 0.4 mm/day and 0.09 mm/day less than other models, respectively. The cold spring would damage the panicle initialization stage of rice and therefore reduce its yield. Also without irrigation, a dry summer and fall would cause water deficiency for rice growth.

Compared with 1pctCO2, simulated average rice production in G2 is 3.0 ± 4.0 Mt (2.4±4.0%) less from year 36 to year 50, and immediately returns back to the level of 1pctCO2 after the end of geoengineering (Table 3). So, on average, climate changes under G2, including the CO_2 fertilization effect, reduce Chinese rice production in our crop simulations. However, models act differently even in terms of the sign of the trend. Two out of 10 models have higher average rice production in the years 36-50 of G2 compared with 1pctCO2, which are BNU-ESM and HadGEM2-ES (Figure 5a). But all the changes are not significant, since they are within the natural variability of rice yield.

The reduction of rice production is due to rice yield decreasing in Northern China (Figure 6a). Simulated temperature reduction due to geoengineering might have a negative impact on rice yield in higher latitude regions in China, while in central and southern China, cooler surface increases the rice yield slightly, but all within the natural variability of the rice yield.

3.3. Maize production changes

Chinese maize production is defined in the same way as rice production in section 3.2. During years 36-50 of the G2 geoengineering scenario, simulated maize production decreases by 17.2±10.6 Mt as compared to the control run (Figure 7a), but increases by 18.1±6.0 Mt as compared to 1pctCO2 (Figure 7b). Those increases in all models are statistically significant except for CCSM-CAM4. Figure 6b shows the spatial distribution of maize yield changes. Maize is very sensitive to temperature change, and prefers a cooler environment than rice. Therefore, as a result of the crop simulations, SRM has the strongest positive impact in

Northern China, and Southern China shows less maize yield increase. Hainan (province 8) is the only region with maize yield reduction, but this reduction is negligible with a value of -0.2%. After the termination of geoengineering in G2, all models show the same decreasing trend (Figures 5c and 5d) ranging from 11.4 Mt (7.6%) (NorESM1-M) to 29.4 Mt (17.7%) (MPI-ESM-LR) with an average of 19.6 Mt (11.9%). This yield reduction is more than the maize yield natural variability for 7 models (BNU-ESM, CESM-CAM5.1-FV, CCSM-CAM4, HadGEM2-ES, IPSL-CM5A-LR, MIRCO-ESM and MPI-ESM-LR). The simulated rapid temperature increasing after the end of geoengineering quickly shows a negative impact on maize growth. However, maize yield is still 6.1 Mt higher than that of the level of 1pctCO2 even after the end of geoengineering (Figures 7a and 7b).

3.4. CO_2 fertilization effect

An elevated CO_2 concentration would directly increase photosynthetic carbon gain for C3 plants such as rice [e.g., *Allen et al.*, 1987] and decrease stomatal conductance of CO_2 and water vapor, which could maintain canopy carbon gain during dry periods for both C3 and C4 (e.g., maize) plants [*Leakey et al.*, 2009]. Although rising CO_2 concentration does not necessarily lead to an increase of crop yield, especially for C4 crops such as maize [e.g., *Long et al.*, 2004], the CO_2 fertilization effect is considered a key climate factor to compensate for the negative effect of global warming on agriculture [e.g., *Parry et al.*, 2004]. In DSSAT v4.5, the CO_2 fertilization effect is parameterized with a fixed nonlinear function for different crops. For example, the CO_2 fertilization effect for maize is 1.00 when CO_2 concentration is 330 ppm, and it is 1.10 when CO_2 concentration is doubled [*Hoogenboom et al.*, 2010].

Without the CO_2 fertilization effect in G2, both simulated rice and maize production decreased (Figures 8a and 8b). With the increase of CO_2 concentration by 1% per year in G2, the CO_2 fertilization effect increased Chinese rice production from 7.5 Mt (8.5% of G2 with constant CO_2 concentration of 409 ppm) in year 36 to 11.3 Mt (12.9%) in year 65 and

Chinese maize production from 7.3 Mt (4.8%) in year 36 to 8.0 Mt (5.7%) in year 65. For rice, the CO_2 fertilization effect opposes the effects due to climate changes in G2. Simulated SRM climate changes tend to reduce rice production by 11.6±6.8 Mt as compared to 1pctCO2, while the CO_2 fertilization effect raises rice production by 8.6 Mt. Therefore, the reduction of rice production in G2 due to temperature and precipitation change is countered by rising CO_2 concentration. This result is consistent with *Pongratz et al.* [2012], who found that rice production would slightly decrease under a 2×CO_2 geoengineered world compared to 2×CO_2 non-geoengineered scenario due to the combination effect of climate changes and the CO_2 fertilization effect in middle latitudes of Northern Hemisphere. For maize, the CO_2 fertilization effect and simulated G2 geoengineering climate changes both increase production, with CO_2 contributing 42.2% of the maize production increase during the last 15 years of G2 geoengineering. This finding is consistent with *Pongratz et al.* [2012], which showed ~50% CO_2 fertilization effect contributing to maize yield increase. Since *Pongratz et al.* [2012] used the CO_2 fertilization factors from the DSSAT model, this is not surprising, and other treatments of this relatively poorly constrained effect would likely give different results, such as shown in Figure 3 of *Jones et al.* [2013].

3.5. Dependence of Results on Climate Factors

To determine which variables were the most important in influencing the results, we conducted a linear regression analysis for rice and maize at each location under the G2 and 1pctCO2 scenarios. The regression uses 900 years of seasonal climate factors as variables and crop yield as predictor. The 13 climate variables are three seasons (spring, summer, and fall) of maximum temperature, minimum temperature, precipitation, and solar radiation, and annual CO_2 concentration In total, there are 25 (locations) × 10 (models) equations for each crop under each scenario (G2 and 1pctCO2). Then we counted total number of *p*-values less than 0.05 for each variable to indicate its significance.

Summer and fall precipitation are the most significant for crop yield (Figure 9). In particular, fall precipitation is considered significant in 55% of the predictions of crop yield. Because we turned off the irrigation function in our simulations, precipitation is the only water source for crops; either drought or flood would cause failure of crop growth. For example, the precipitation deficiency in year 49 simulated by HadGEM2-ES caused a drop in production in both rice and maize. For maize, summer maximum temperature is also important in more than half of the cases. G2 geoengineering produced a cooler surface, therefore alleviating heat stress and significantly increasing maize production. The differences of factor significance between G2 and 1pctCO2 scenarios for both rice and maize are not significant.

3.6. Uncertainties

There are several uncertainties in this study. Different SRM techniques could bring different climate responses [*Niemeier et al.*, 2013], which will impact agriculture in a totally different way. In this study, we just focus on one of the experiments designed in GeoMIP (G2), and since ten climate modeling groups did the same experiment, we have a relatively robust climate response in term of this specific SRM scenario.

The downscaling method could make a big difference in an agriculture impact study. The delta method with or without variability correction, and bias correction with or without variability are all simple, and commonly used downscaling methods. Although the delta method without variability correction is likely a good way to create temperature input [*Hawkins et al.*, 2013], several difficulties arise when using this method to create precipitation forcing. Different patterns of precipitation (event intensity and event duration) with the same average monthly precipitation value could significantly alter the results, especially because in our analysis we found that spring and summer precipitation are the most

important factors controlling rice and maize production. A change of precipitation pattern from using a different downscaling technique might change our results.

Insufficient agriculture practice data, such as planting dates in different provinces and details of different cultivars used in regions, would affect model evaluation and the details of our results. In addition, crop yield reports might not be accurate due to human error.

Other important climate factors affecting rice and maize production have not been considered in this study, such as changes in ultraviolet radiation and diffuse solar radiation. These are important factors to consider in future studies using stratospheric sulfate injection geoengineering scenarios. In addition, the CO_2 fertilization effect is parameterized in DSSAT, and this fixed value determines how CO_2 concentration contributes to crop yield. More recent understanding of the CO_2 fertilization effect on different crops [e.g., *Lam et al.*, 2013; *Nam et al.*, 2013] might the improve crop simulation.

Different crop models produce a range of crop yield predictions under the same climate forcing and the same agricultural management [*Palosuo et al.*, 2011; *Rotter et al.*, 2011]. An intercomparison of the response of several different crop models to geoengineering would be valuable in the future.

4. Conclusions

Using the climate changes due to SRM as simulated by 10 climate models (GeoMIP G2), Chinese simulated rice production falls by 3.0±4.0 Mt (2.4±4.0%) during the last 15 years of geoengineering (years 36-50) as compared with rice production in the 1pctCO2 run, due to the combined effects of the simulated climate changes and the CO_2 fertilization. Without the benefit of rising CO_2, our simulations show that Chinese rice production drops 11.6±6.8 Mt (11.6±6.8%) as compared to 1pctCO2. The termination effect from SRM raises Chinese rice production by 5.2 Mt in the first 15 years of a post-geoengineering period (years 51-65) compared with rice production during the last 15 years of geoengineering (years 36-

50), back to the level of 1pctCO2. In particular, if CO_2 concentrations continue to increase in the simulation, the CO_2 fertilization effect would compensate for the negative effect from geoengineering climate changes in simulations. However, all of these changes are within the natural variability of rice production in China. Therefore, based on the rice simulations, G2 geoengineering has no significant effect on Chinese rice production.

In our model, maize production in China benefits from SRM (GeoMIP G2) with an increased production of 18.1±6.0 Mt (13.9±5.9%) compared with that in a 1pctCO2 scenario during the years 36-50, with the combination of effects of climate and the CO_2 fertilization effect. Climate changes in G2, in particular the relief of heat stress, contributes to 58% of this maize production increase, and high CO_2 concentration contributes to the remaining 42%, raising maize production by around 7.7 Mt. When geoengineering ceases, the consequent rapid temperature rise causes simulated maize production to decrease to the level of that in 1pctCO2 within one year, implying serious consequences for local and national food security.

Non-irrigated agriculture depends strongly on precipitation amounts. Summer and spring precipitation are significant for rice and maize production based on a linear regression analysis in our study. At some locations in several climate models, G2 geoengineering reduced the mean precipitation but with a larger variability. Therefore, local climate variations with interchanging droughts and floods would damage crop yields, and also make precipitation in the growing season an important factor controlling agriculture production. Temperature is another essential factor controlling crop production. Heat stress due to the climate response to the greenhouse gas forcing would be harmful for most of the crops although the CO_2 fertilization effect could partially compensate for this negative impact, especially for C3 plants such as rice. The aim of geoengineering would be to cool Earth to help address the problem of global warming. As such, the cooling effect of geoengineering would benefit the current agricultural yield, particularly for maize, although there are other

climate changes from SRM geoengineering simulations, such as an increase in incident ultraviolet light, that might harm agriculture. In addition, all analysis is based on current agriculture practices and cultivars; with the development of heat resistant crops, they might be less sensitive to the temperature changes.

Although this study benefits from GeoMIP with 10 climate models' simulations of the same geoengineering experiment, we only used one geoengineering scenario, one simple downscaling method, one crop model, two crops, and one region. Clearly, further investigation is needed, including on global agricultural response and on the world trade system, to understand how food security would be impacted by geoengineering.

Acknowledgments. We thank the reviewers, particularly Julia Pongratz, for valuable suggestions that helped to improve the paper. We thank all participants of the Geoengineering Model Intercomparison Project and their model development teams, the CLIVAR/WCRP Working Group on Coupled Modeling for endorsing GeoMIP, and the scientists managing the Earth System Grid data nodes who have assisted with making GeoMIP output available. We acknowledge the World Climate Research Programme's Working Group on Coupled Modelling, which is responsible for CMIP, and we thank the climate modeling groups for producing and making available their model output. For CMIP, the U.S. Department of Energy's Program for Climate Model Diagnosis and Intercomparison provides coordinating support and led development of software infrastructure in partnership with the Global Organization for Earth System Science Portals. Lili Xia and Alan Robock are supported by NSF grants AGS-1157525 and GEO-1240507. Andy Jones was supported by the Joint DECC/Defra Met Office Hadley Centre Climate Programme (GA01101), the IAGP programme (http://www.iagp.ac.uk) and the SPICE program (http://www2.eng.cam.ac.uk/~hemh/climate/Geoengineering_RoySoc.htm). Shingo

Watanabe was supported by SOUSEI program, MEXT, Japan, and his simulations were performed using the Earth Simulator. Ulrike Niemeier received funding from the European Commission's Seventh Framework Programme through the IMPLICC project (FP7-ENV-2008-1-226567). Helen Muri is supported by EU 7th Framework Programme grant no. 306395 (EuTRACE). Ben Kravitz is supported by the Fund for Innovative Climate and Energy Research. The Pacific Northwest National Laboratory is operated for the U.S. Department of Energy by Battelle Memorial Institute under contract DE-AC05-76RL01830. Simulations performed by Ben Kravitz were supported by the NASA High-End Computing Program through the NASA Center for Climate Simulation at Goddard Space Flight Center. Simone Tilmes is supported by NSF.

References

Aleinov, I. and G. Schmidt (2006), Water isotopes in the GISS ModelE land surface scheme, *Glob. Plan. Change*, *51*(1-2), 108-120, doi:10.1016/j.gloplacha.2005.12.010.

Allen Jr, L. H., K. J. Boote, J. W. Jones, P. H. Jones, R. R. Valle, B. Acock, H. H. Rogers and R. C. Dahlman (1987), Response of vegetation to rising carbon dioxide: Photosynthesis, biomass, and seed yield of soybean, *Global Biogeochemical Cycles*, *1*(1), 1-14, doi:10.1029/GB001i001p00001.

Arora, V. K., et al. (2011), Carbon emission limits required to satisfy future representative concentration pathways of greenhouse gases, *Geophys.Res. Lett.*, *38*, L05805, doi:10.1029/2010GL046270.

Arora, V. K. and G. J. Boer (2010), Uncertainties in the 20th century carbon budget associated with land use change, *Glob. Change Biol.*, *16*(12), 3327-3348, doi:10.1111/j.1365-2486.2010.02202.x.

Batjes, N. H. (2008), ISRIC-WISE Harmonized Global Soil Profile Dataset (Ver. 3.1). Report 2008/02, ISRIC - World Soil Information, Wageningen (with dataset), http://www.isric.org/isric/Webdocs/Docs/ISRIC_Report_2008_02.pdf.

Batjes, N. H. (2009), Harmonized soil profile data for applications at global and continental scales: updates to the WISE database, *Soil Use and Management*, *25*, 124-127, doi: 10.1111/j.1475-2743.2009.00202.x.

Bentsen, M., et al. (2013). The Norwegian Earth System Model, NorESM1-M – Part 1: Description and basic evaluation of the physical climate. *Geosc. Model Dev.*, *6*(3), 687–720.

Collins, W. J., et al. (2011), Development and evaluation of an Earth-System model-HadGEM2, *Geosci. Model Dev.*, *4*, 1051-1075, doi:10.5194/gmd-4-262728.

Crutzen, P. (2006), Albedo enhancement by stratospheric sulfur injections: A contribution to resolve a policy dilemma?, *Climatic Change*, *77*(3), 211-220, doi: 10.1007/s10584-006-9101-y.

Curry, C. L., et al. (2014), A multi-model examination of climate extremes in an idealized geoengineering experiment. Submitted to *J. Geophys. Res. Atmos.*, doi:10.1029/ 2013JD020648.

Dai, M., H. Tao, S. Liao, L. Wang, and P. Wang (2008), Estimation and analysis of maize potential productivity based on CERE-Maize model in the North China Plain, *Transactions of the CSAE*, *24*, 30-36.

Dufresne, J.-L., et al. (2013), Climate change projections using the IPSL-CM5 Earth System Model: From CMIP3 to CMIP5, *Clim. Dyn.*, *40*, 2123-2165, doi:10.1007/s00382-012-1636-1.

Essery, R. L. H., M. J. Best, R. A. Betts, P. M. Cox, and C. M. Taylor (2003), Explicit representation of subgrid heterogeneity in a GCM land surface scheme, *J. Hydrometeorol.*, *4*, 530-543, doi:10.1175/1525-7541(2003)004<0530:EROSHI>2.0.CO;2.

Fan, M., W. Wu, and H. Liu (2010), Optimization and Validation of Genetic Parameters of Maize Based on CERES-Maize Model, *Journal of Anhui Agri. Sci.*, *38*(6), 3087-3089.

FAO (2012) , FAO statistical yearbook 2010. Food and Agriculture Organization of the United Nations. http://www.fao.org/economic/ess/ess-publications/ess-yearbook/yearbook2012/en/.

Gent, P. R., et al. (2011), The Community Climate System Model 4, *J. Clim.*, *24*, 4973-4991, doi:10.1175/2011JCLI4083.1.

Giorgetta, M. A., et al. (2013), Climate and carbon cycle changes from 1850 to 2100 in MPI-ESM simulations fro the Coupled model Intercomparison Project phase 5, *JAMES*, *5* (3), 572-597, doi:10.1002/jame.20038..

Govindasamy, B., and K. Caldeira (2000), Geoengineering Earth's radiation balance to mitigate CO2-induced climate change, *Geophys. Res. Lett*., *27*, 2, 141-2, 144, doi:10.1029/1999GL006086.

HadGEM2 Development Team (2011), The HadGEM2 family of Met Office Unified Model climate configurations, *Geosci. Model Dev.*, *4*, 723-757, doi:10.5194/gmd-4-723-2011.

Hawkins, E., T. M. Osborne, C. K. Ho, and A. J. Challinor (2013), Calibration and bias correction of climate projections for crop modeling: An idealised case study over Europe, *Ag. Forest Meteorology*, *170*, 19-31, doi:10.1016/j.agrformet.2012.04.007.

Hoogenboom, G., J. W. Jones, C. H. Porter, P. W. Wilkens, K. J. Boote, L. A. Hunt, and G. Y. Tsuji (Editors) (2010), Decision Support System for Agrotechnology Transfer Version 4.5. Volume 1: Overview. University of Hawaii, Honolulu, HI.

Hoogenboom, G., J. W. Jones, P. W. Wilkens, C. H. Porter, K. J. Boote, L. A. Hunt, U. Singh, J. L. Lizaso, J. W. White, O. Uryasev, F. S. Royce, R. Ogoshi, A. J. Gijsman, G. Y. Tsuji, and J. Koo, (2012), Decision Support System for Agrotechnology Transfer (DSSAT) Version 4.5 [CD-ROM]. University of Hawaii, Honolulu, Hawaii.

Hourdin, F., et al. (2013), Impact of the LMDZ atmospheric grid configuration on the climate and sensitivity of the IPSL-CM5A coupled model, *Clim. Dynam.*, *40*, 2167-2192, doi:10.1007/s00382-012-1411-3.

Ji, D., et al. (2014), Description and basic evaluation of BNU-ESM version 1, *Geosci. Model Dev. Discuss.*, *7*, 1601-1647, doi:10.5194/gmdd-7-1601-2014.

Jones, A., J. Haywood, O. Boucher, B. Kravitz, and A. Robock, 2010: Geoengineering by stratospheric SO_2 injection: Results from the Met Office HadGEM2 climate model and comparison with the Goddard Institute for Space Studies ModelE. *Atmos. Chem. Phys.*, *10*, 5999-6006, doi:10.5194/acp-10-5999-2010.

Jones, A., et al. (2013), The impact of abrupt suspension of solar radiation management (termination effect) in experiment G2 of the Geoengineering Model Intercomparison Project (GeoMIP). *J. Geophys. Res. Atmos.*, *118*, 9743-9752, doi:10.1002/jgrd.50762.

Jones, J. W., et al. (2003), The DSSAT cropping system model. *Eur J Agron*, *18* (3-4):235-265. doi:10.1016/S1161-0301(02)00107-7.

K-1 model developers (2004), K-1 Coupled GCM (MIROC) Description, K-1 Technical Report No. 1 (Center for Climate System Research, National Institute for Environmental Studies, and Frontier Research Center for Global Change), available online at http://www.ccsr.u-tokyo.ac.jp/kyosei/hasumi/MIROC/tech-repo.pdf.

Kravitz, B., A. Robock, O. Boucher, H. Schmidt, K. E. Taylor, G. Stenchikov, and M. Schulz (2011), The Geoengineering Model Intercomparison Project (GeoMIP), *Atmos. Sci. Lett.*, *12*(2), 162-167, doi:10.1002/as1.316.

Krinner, G., et al. (2005), A dynamic global vegetation model for studies of the coupled atmosphere-biosphere system, *Global Biogoechem.Cyc.*, *19*, GB1015, doi:10.1029/2003GB002199.

Lam, S. K., D. Chen, R. Norton, and R. Armstrong (2013), The effect of elevated atmospheric carbon dioxide concentration on the contribution of residual legume and fertilizaer nitrogen to a subsequent wheat crop, *Plant and Soil*, *364*(1-2), 81-91, doi:10.1007/s11104-012-1314-4.

Leakey, A. D. B., E. A. Ainsworth, C. J. Bernacchi, A. Rogers, S. P. Long, and D. R. Ort (2009), Elevated CO_2 effects on plant carbon, nitrogen, and water relations: Six important lessons from FACE, *J. Exp. Bot.*, *60*(10), 2859-2876, doi:10.1093/jxb/erp096.

Lobell, D. B., W. Schlenker, and J. Costa-Roberts (2011), Climate trends and global crop production since 1980, *Science*, *333*(6042), 616-620, doi:10.1126/science.1204531.

Long, S. P., E. A. Ainsworth, A. Rogers, and D. R. Ort (2004), Rising atmospheric carbon dioxide: Plants face the future, *Annu. Rev. Plant. Biol.*, *55*, 591-628, doi:10.1146/annurev.arplant.55.031903.141610.

Long, S. P., E. A. Ainsworth, A. D. B. Leakey, J. Nosberger, and D. R. Ort (2006), Food for thought: Lower-than-expected crop yield stimulation with rising CO_2 concentrations, *Science*, *312*(5782), 1918-1921, doi:10.1126/science.1114722.

Madec, G. (2008), *NEMO ocean engine.* Tech. Rep. 27, Institut Pierre Simon Laplace des Sciences d l'Environement Global (Paris).

Matthews, H. D. and K. Caldeira (2007), Transient climate-carbon simulations of planetary geoengineering, *PNAS*, *104*, 24, 9949-9954, doi:10.1073/pnas.0700419104.

Ministry of Agriculture of the People's Republic of China (2009), *60 years of Agriculture of the People's Republic of China*. China Agriculture Press, Beijing, China.

Nam, H. S., et al. (2013), Fertilizer N uptake of paddy rice in two soils with different fertility under experimental warming with elevated CO_2, *Plant Soil*, *369*, 563-575, doi:10.1007/s11104-013-1598-z.

Niemeier, U., H. Schmidt, K. Alterskjær, and J. E. Kristjánsson (2013), Solar irradiance reduction via climate engineering – Impact of different techniques on the energy balance and the hydrological cycle, *J. Geophys. Res. Atmos.*, *118*, 11,905-11,917, doi:10.1002/2013JD020445.

Palosuo, T., et al. (2011), Simulation of winter wheat yield and its variability in different climates of Europe: A comparison of eight crop growth models, *Eur. J. Agron.*, *35*(3), 103-114, doi:10.1016/j/eja.2011.05.001.

Parry, M. L., C. Rosenzweig, A. Iglesias, M. Livermore, and G. Fischer (2004), Effects of climate change on global food production under SRES emissions and socio-economic scenarios, *Global Environmental Change*, *14*, 53-67, doi:10.1016/j.gloenvcha.2003.10.008.

Pongratz, J., D. B. Lobell, L. Cao, and K. Caldeira (2012), Crop yields in a geoengineered climate, *Nature Clim. Change*, *2*(2), 101-105, doi:10.1038/nclimate1373.

Rasch, P. J., et al. (2008), An overview of geoengineering of climate using stratospheric sulphate aerosols. *Phil. Trans. Royal Soc. A.*, *366*, 4007-4037, doi:10.1098/ rsta.2008.0131.

Robock, A. (2008), 20 reasons why geoengineering may be a bad idea, *Bull. Atomic Scientists*, *64* (2), 14-18, doi:10.2968/064002006.

Robock, A., L. Oman, and G. Stenchikov (2008), Regional climate responses to geoengineering with tropical and Arctic SO_2 injections, *J. Geophys. Res.*, *113*, D16101, doi:10.1029/2008JD010050.

Rosenzweig, C., M. L. Parry (1994), Potential impact of climate change on world food supply. *Nature*, *367*(13), 133-138.

Rötter R. P., T. R. Carter, J. E. Olesen, and J. R. Porter (2011), Crop-climate models need an overhaul, *Nature Clim. Change*, *1*(4), 175-177, doi:10.1038/nclimate1152.

Russell, G. L., J. R. Miller, and D. Rind (1995), A coupled atmosphere-ocean model for transient climate change, *Atmos.-Ocean*, *33*, 683-730.

Schmidt, G. A., et al. (2006), Present-day atmospheric simulations using GISS ModelE: Comparison to in situ, satellite and reanalysis data, *J. Clim.*, *19*, 153–192, doi:10.1175/JCLI3612.1.

Smith, R. D. et al. (2010), *The Parallel Ocean Program (POP) Reference Manual*, Los Alamos National Laboratory Tech. Rep. LAUR-10-1853.

Stevens, B., et al. (2013), The atmospheric component of the MPI-M Earth system model:ECHAM6, *J. Adv. Model. Earth Syst.*, *5*, 146-172, doi:10.1002/jame.20015.

Takata, K., S. Emori, and T. Watanabe (2003), Development of the minimal advanced treatments of surface interaction and runoff, *Glob. Plan. Change*, *38*(1-2), 209-222, doi:10.1016/S0921-627!8181(03)00030-4.

Taylor, K. E., R. J. Stouffer, and G. A. Meehl (2012), An Overview of CMIP5 and the Experiment Desgin, *Bull. Amer. Meteor. Soc.*, *93*, 485-498, doi:http://dx.doi.org/10.1175/BAMS-D-11-00094.1.

Verseghy, D., N. A. McFarlane, and M. Lazare (1993), CLASS–A Canadian land surface scheme for GCMs, II: Vegetation model and coupled runs, *Int. J. Climatol.*, *13*, 347-370.

Watanabe, S., et al. (2008), Development of an atmospheric general circulation model for integrated Earth system modeling on the Earth Simulator, *J. Earth Simulator*, *9*, 27-35.

Watanabe, S., et al. (2011), MIROC-ESM 2010: Model description and basic results of CMIP5-20c3m experiments, *Geosci. Mod. Dev.*, *4*, 845-872, doi:10.5194/gmd-4-845-2011.

Wigley, T. M. L. (2006), A combined mitigation/geoengineering approach to climate stabilization, *Science*, *314*, 452-454, doi:10.1126/science.1131728.

Xia, L., and A. Robock (2013), Impacts of a nuclear war in South Asia on rice production in Mainland China, *Climatic Change*, *116*(2), 357-372, doi:10.1007/s10584-012-0475-8.

Yao, F. M., Y. L. Xu, E. D. Lin, M. Yokozawa, and J. H. Zhang (2007), Assessing the impacts of climate change on rice yields in the main rice areas of China, *Climatic Change*, *80* (3-4):395-409. doi: 10.1007/s10584-006-9122-6.

Zhang, Y., Y. Ma, and S. Liao (2004) Method of optimizing maize variety parameters in the CERES-maize simulation model, *Journal of China Agricultural University*, *9*(4), 24-29.

Table 1. Province locations and agricultural data used in DSSAT simulations. Numbers refer to province locations in Figure 6. Latitudes, longitudes, and elevations are for weather stations used to force the model for the different crops for the evaluation. Climate model output was also extracted from these locations for the simulations. Crop area and production data are for 2008 [*Ministry of Agriculture of the People's Republic of China*, 2009].

No.	Province	Crop	Latitude (°N)	Longitude (°E)	Altitude (m)	Area (kha)	Production (kt)
1	Anhui	Rice	31.9	117.2	28	1700	11024
		Maize	31.9	117.2	28	705	2866
2	Beijing	Rice	39.8	116.5	31	0.4	3
		Maize	39.8	116.5	31	146	880
3	Fujian	Rice	26.7	118.2	126	2670	437
		Maize	24.5	118.1	139	136	37
4	Gansu	Rice	40.3	97.0	1526	6	38
		Maize	40.3	97.0	1526	557	2654
5	Guangdong	Rice	24.7	113.6	61	933	4750
		Maize	22.8	115.4	17	144	635
6	Guangxi	Rice	22.0	108.6	15	151	877
		Maize	25.3	110.3	164	490	2072
7	Guizhou	Rice	26.6	106.7	1224	686	4576
		Maize	27.3	105.3	1511	735	3912
8	Hainan	Rice	20.0	110.3	64	129	650
		Maize	19.1	108.6	8	17	70
9	Hebei	Rice	40.4	115.5	54	82	556
		Maize	39.4	118.9	11	2841	14422
10	Heilongjiang	Rice	44.6	129.6	241	2391	15180
		Maize	48.1	125.9	235	3594	18220
11	Henan	Rice	36.1	114.4	76	605	4431
		Maize	36.1	114.4	76	2820	16150
12	Hubei	Rice	30.3	109.5	457	1228	10892
		Maize	30.3	109.5	457	470	2264
13	Hunan	Rice	26.2	111.6	173	1255	8831
		Maize	27.5	110.0	272	241	1280
14	Jiangsu	Rice	34.3	117.2	41	2228	17688
		Maize	34.9	119.1	3	399	2030
15	Jiangxi	Rice	27.1	114.9	71	401	2680
		Maize	28.6	115.9	47	16	66
16	Jilin	Rice	45.1	124.9	136	659	5790
		Maize	43.9	125.2	236	2923	20830
17	Liaoning	Rice	42.4	122.5	79	659	5056
		Maize	41.5	120.5	170	1885	11890
18	Neimenggu	Rice	43.6	118.1	799	98	705
		Maize	40.2	104.8	1324	2340	14107
19	Ningxia	Rice	38.5	106.2	1111	80	664
		Maize	38.5	106.2	1111	209	1499
20	Shandong	Rice	37.5	117.5	12	131	1104

		Maize	37.5	117.5	12	2874	18874
21	Shaanxi	Rice	33.1	107.0	510	125	831
		Maize	37.4	122.7	48	1157	4836
22	Sichuan	Rice	32.1	108.0	674	2662	20254
		Maize	28.8	104.6	341	1729	8830
23	Tianjin	Rice	39.1	117.1	13	15	105
		Maize	39.1	117.1	13	160	843
24	Yunnan	Rice	25.1	101.3	1301	947	5775
		Maize	25.1	101.3	1301	1326	5296
25	Zhejiang	Rice	29.0	118.9	82	691	5099
		Maize	30.2	120.2	42	26	111

Table 2. The 10 climate models participating in GeoMIP G2.

Models	Pre-industrial	1pctCO2	G2	References
	(Ensemble members/years)			
BNU-ESM	1/558	1/140	3/70	*Ji et al.* [2014]
CESM-CAM5.1-FV	1/50	1/150	1/70	*Smith et al.*, [2010], *Oleson et al.* [2010]
CanESM2	1/295	1/140	3/100	*Arora et al.*[2011], *Arora and Boer* [2010], *Verseghy et al.* [1993]
CCSM-CAM4	1/50	1/155	1/70	*Gent et al.* [2011]
GISS-E2-R	3/70	3/70	3/70	*Schmidt et al.* [2006], *Russell et al.* [1995], *Aleinov and Schmidt* [2006]
HadGEM2-ES	1/576	1/140	3/80	*Collins et al.* [2011], *Essery et al.* [2003], *HadGEM2 Dev. Team* [2011]
IPSL-CM5A-LR	1/1000	1/150	1/70	*Dufresne et al.* [2013], *Hourdin et al.* [2013], *Madec et al.* [2008], *Krinner et al.* [2005]
MIROC-ESM	1/530	1/140	1/70	*Watanabe et al.* [2008, 2011], *Takata et al.* [2003], *K-I Model Dev.* 2004]
MPI-ESM-R	1/185	1/140	1/70	*Giorgetta et al.* [2013], *Stevens et al.* [2013]
NorESM1-M	1/415	1/140	1/70	*Bentsen et al.* [2013]

Table 3. Crop production changes (Mt) due to G2 geoengineering.

Crop	**G2 - Control**		**G2 - 1pctCO2**		**G2 - G2$_{(CO2 = 409\ ppm)}$**		**G2(yr 51-65) - G2(yr 36-50)**
	yr 36-50	yr 51-65	yr 36-50	yr 51-65	yr 36-50	yr 51-65	
Rice	-7.0	-1.8	-3.0	0.0	8.6	10.3	5.2
Maize	-17.2	-36.7	18.1	6.1	7.7	7.3	-19.6

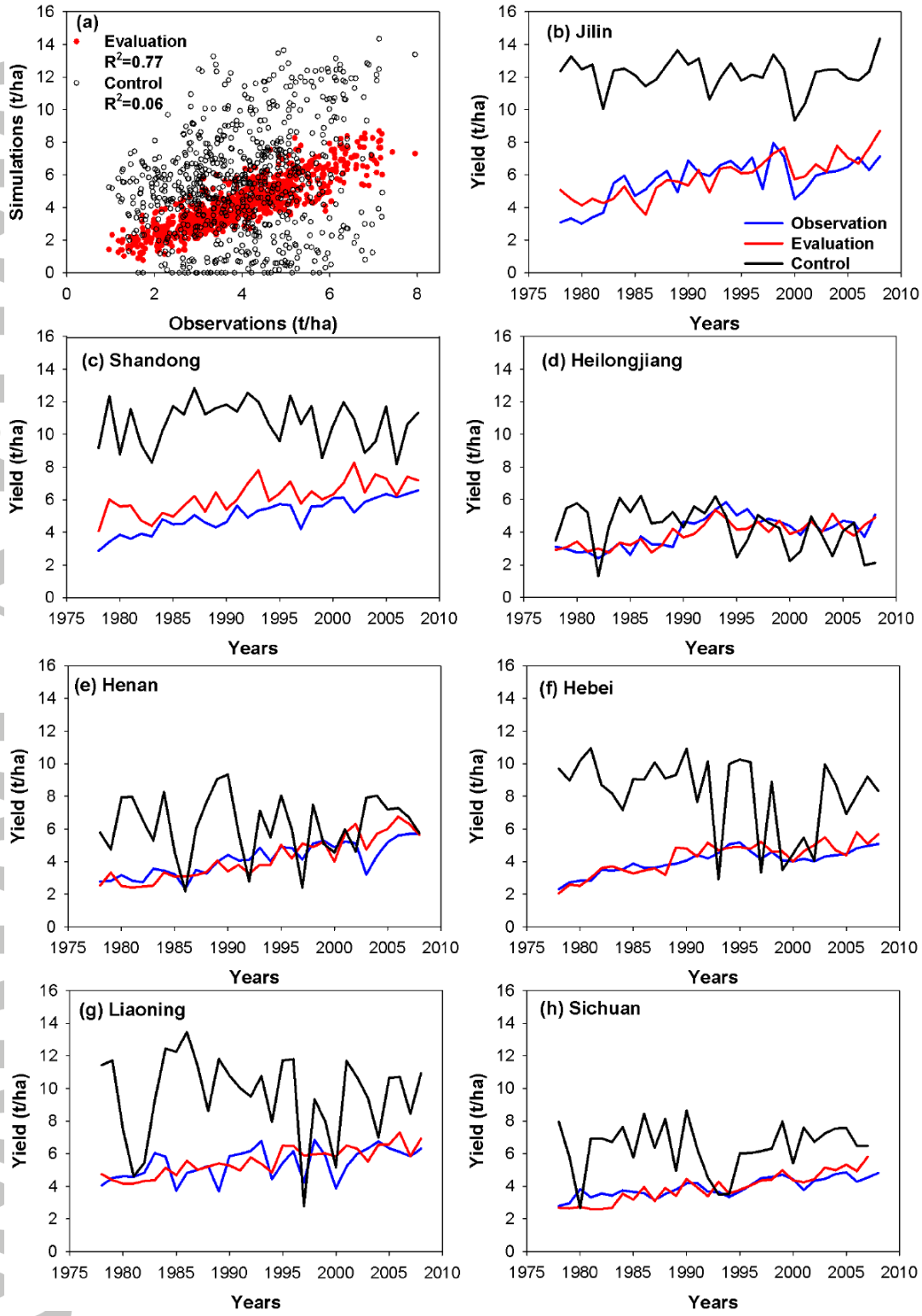

Figure 1. Comparison of DSSAT simulated maize yields (evaluation and control) and observations [t/ha] for the major maize production provinces. Evaluation simulations were forced by recorded agriculture practice, observed monthly CO_2 concentrations and observed daily weather, while control simulations were forced by fixed agriculture practice (150 kg/ha fertilizer, no irrigation), fixed CO_2 concentration and observed daily weather. R^2 is the coefficient of determination. Also shown are time series (1979-2007) of simulated maize yields (evaluation and control) and observations for the top seven maize production provinces: (b) Jilin, (c) Shandong, (d) Heilongjian, (e) Henan, (f) Heibei, (g) Liaoning and (h) Sichuan.

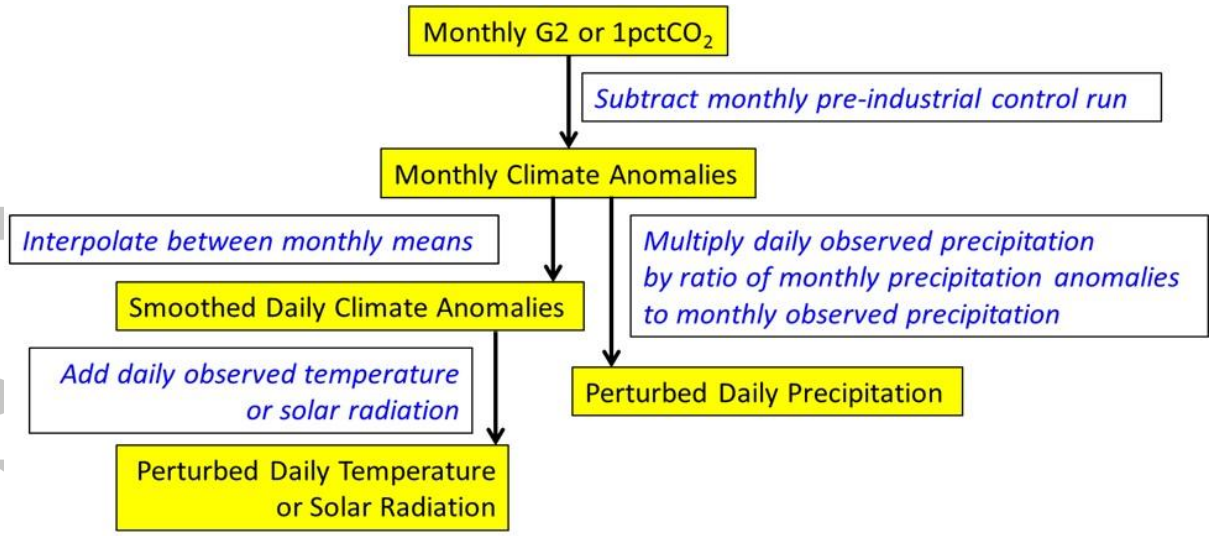

Figure 2. Delta method flow chart describing the downscaling method to create climate input for DSSAT. Monthly pre-industrial control run is the average of all control run years.

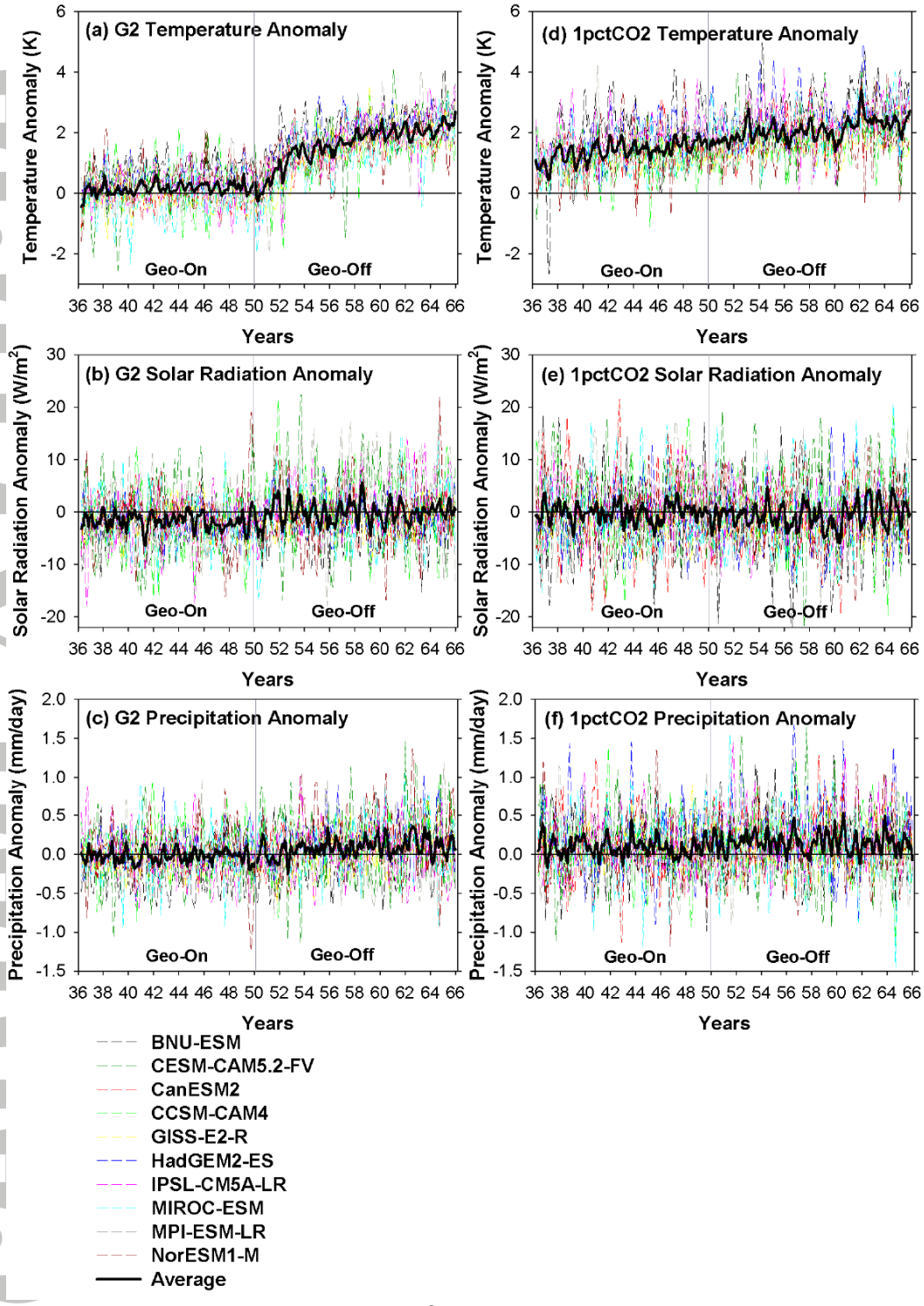

Figure 3. Three-month moving average of monthly climate anomalies (temperature, surface downwelling solar radiation, and precipitation) from GeoMIP G2 and 1pctCO2 starting from the 36th year of solar radiation management and ending at year 65, which is the 15th year after the termination of geoengineering. Colored dashed lines are climate anomalies from the 10 climate models. They are the average of all 42 locations in China. Bold black lines are the average of the 10 models' climate anomalies. The vertical gray lines indicate the end of G2 geoengineering. Temperature anomalies are calculated from the average of maximum temperature and minimum temperature. The left panels (a, b, and c) are differences between G2 and pre-industrial control run, and the right panels (d, e, and f) are differences between 1pctCO2 and the pre-industrial control run.

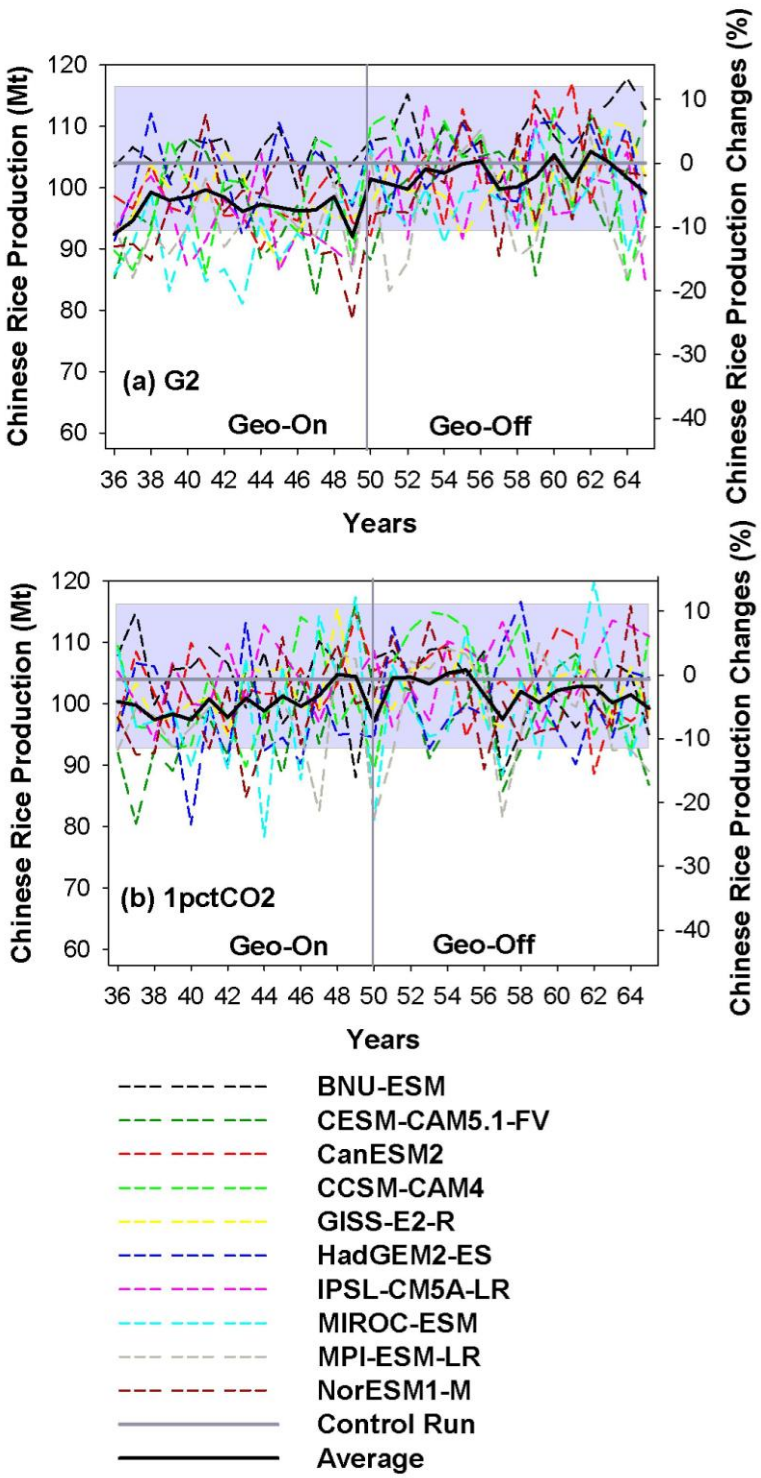

Figure 4. Chinese rice production (Mt) and percentage changes in G2 (a) and 1pctCO2 (b). Since we assume geoengineering starting in 2020 (year 1), year 36 is actually 2055. Colored dashed lines are rice production curves simulated with climate anomalies from the 10 climate models. The bold black lines are the average of the 10 models. The error bars are one standard deviation of rice production simulated from climate forcing of 10 climate models including 30 climate conditions for each year. The bold horizontal gray lines are rice production of the control run. The vertical gray lines indicate the end of G2 geoengineering. The gray area shows one standard deviation from the control runs, illustrating the effect of climate variability.

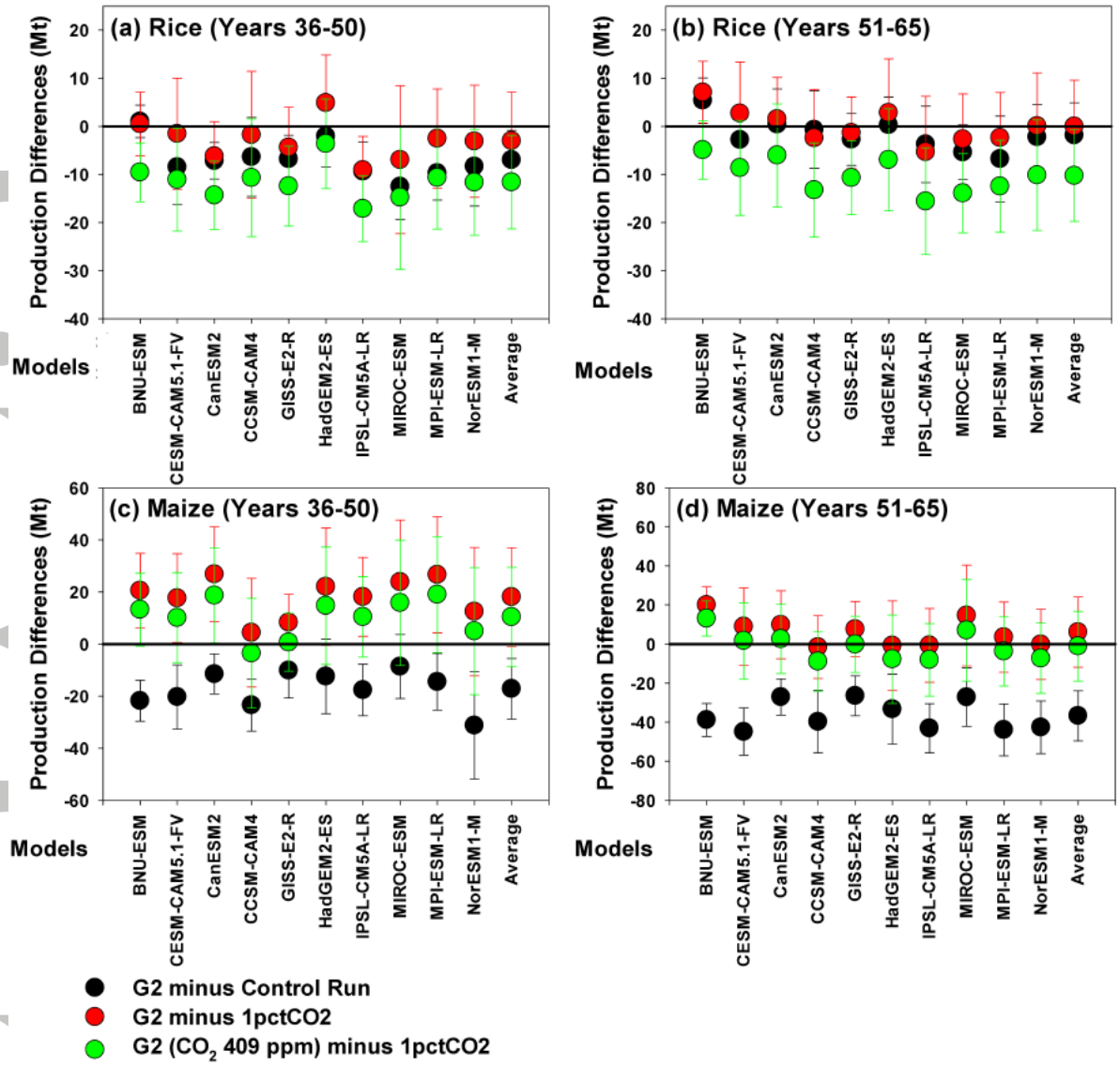

Figure 5. Fifteen-year average crop production changes for rice (a, b) and maize (c,d) of 10 climate models and their average. Error bars are one standard deviation of crop production changes in 15 years.

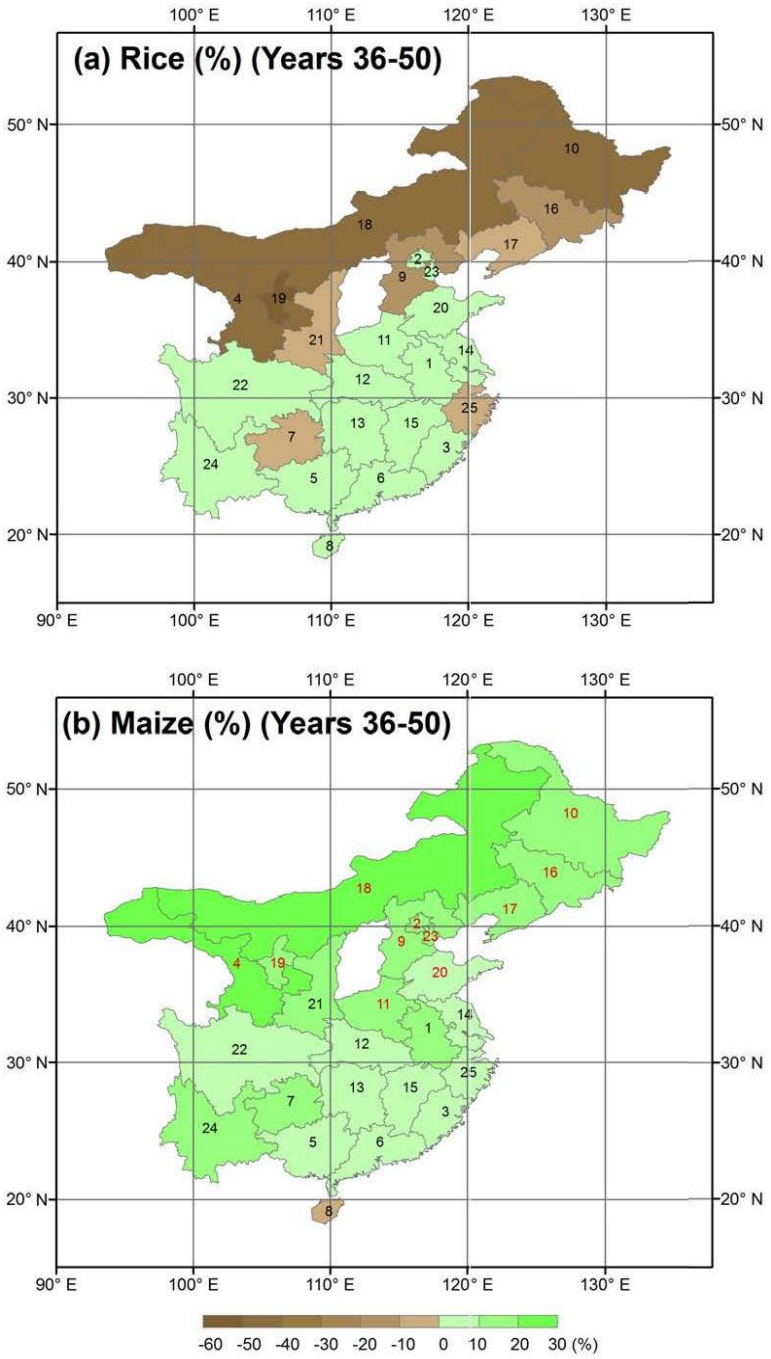

Figure 6. Crop yield changes under simulated G2 geoengineering scenarios (Years 36-50) compared with the same period of 1pctCO2. The yield changes are the average of 10 simulations using 10 climate model output over the 15 years of geoengineering. Green color indicates positive change and brown color indicates negative impact. Province colored means that we did conduct simulations there. The numbers correspond to the names of the different provinces listed in Table 1. In (b), red numbers indicate summer maize and black numbers are spring maize.

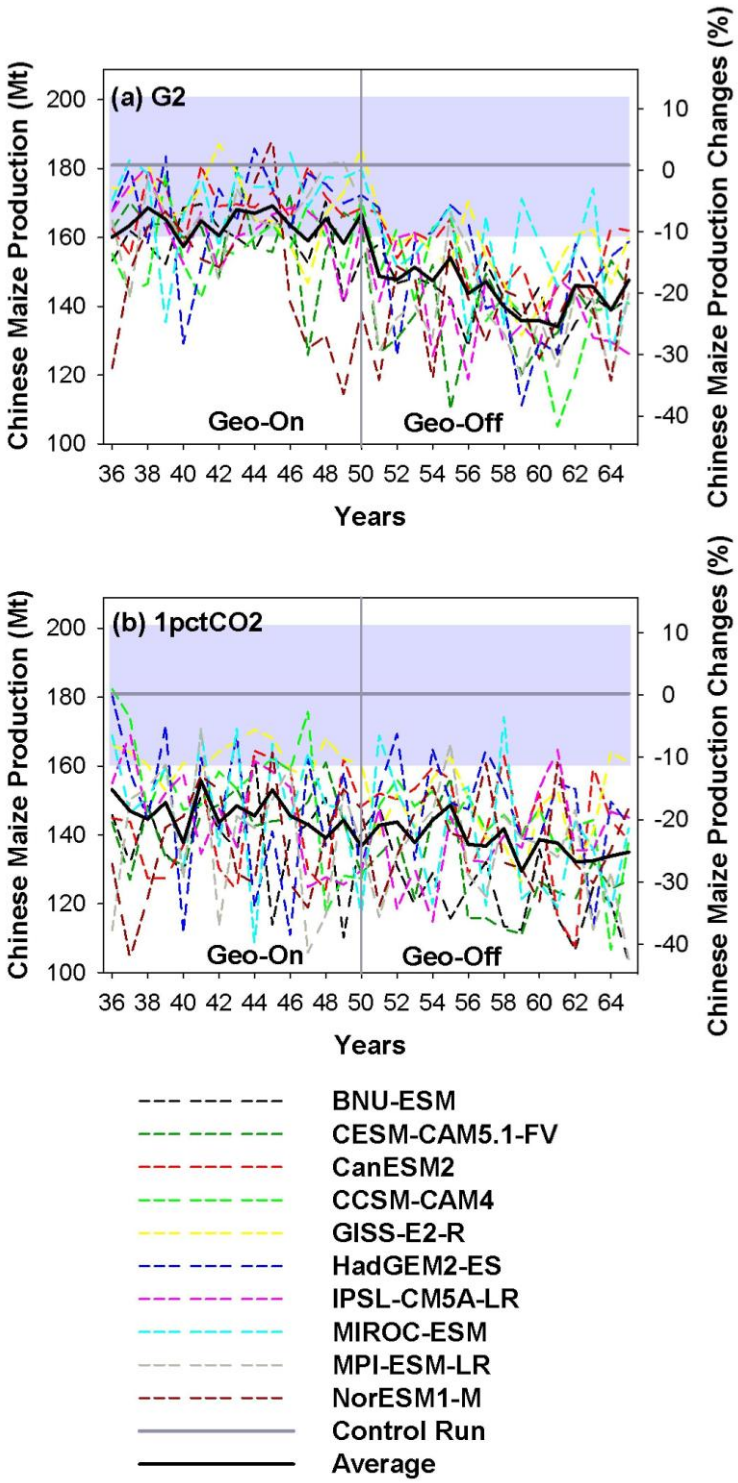

Figure 7. Chinese maize production and percentage changes in G2 (a) and 1pctCO2 (b). Since we assume geoengineering starting in 2020 (year 1), year 36 is actually 2055. Ten colored dashed lines are maize production curves simulated with climate anomalies from the 10 climate models. The bold horizontal gray lines are the model averages. The vertical gray lines indicate the end of G2 geoengineering. The error bars are one standard deviation of maize production simulated from the climate forcing of the 10 climate models including 30 climate conditions for each year. The bold gray lines are maize production of the control run. The gray area shows one standard deviation from the control runs, illustrating the effect of climate variability.

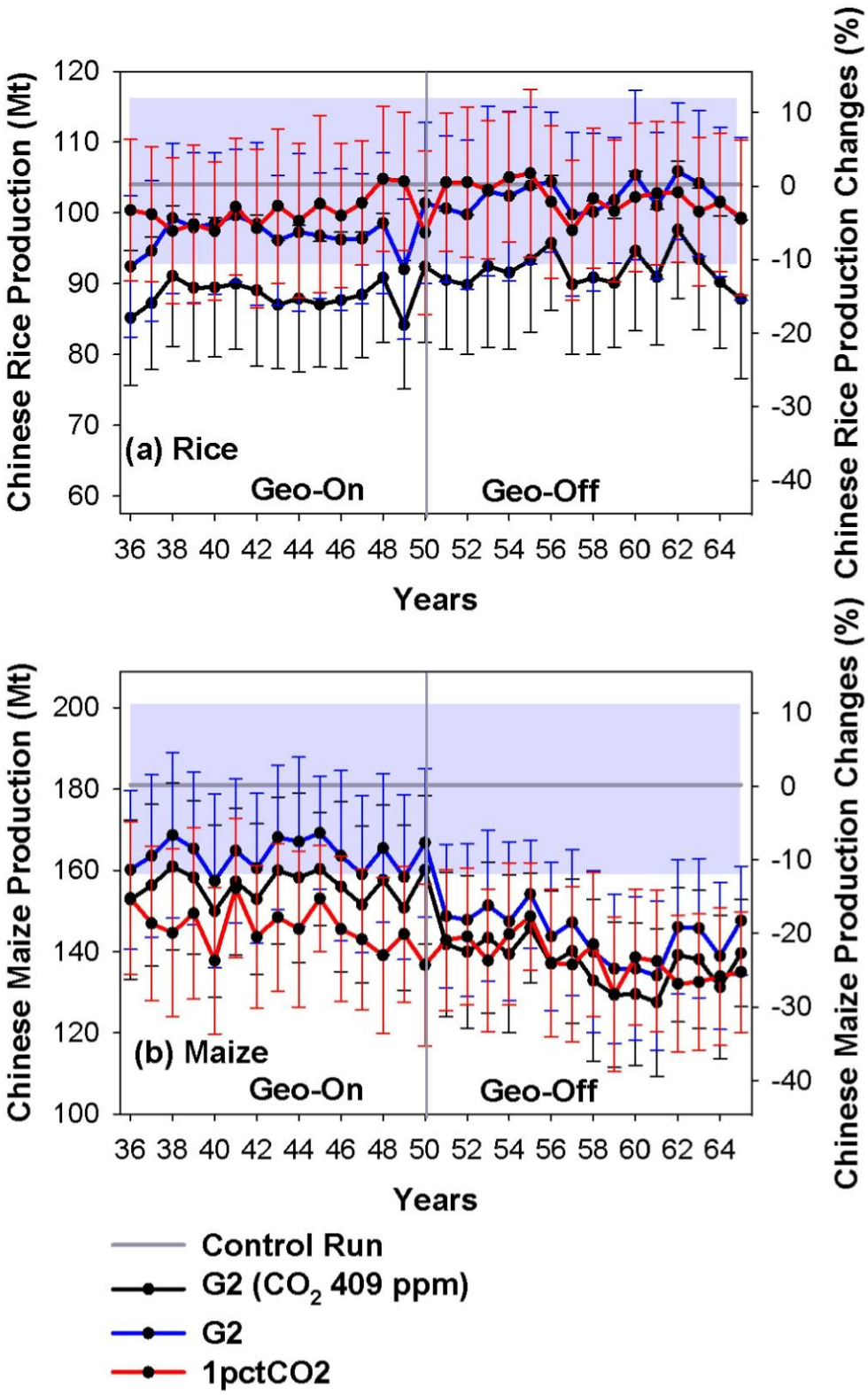

Figure 8. CO_2 fertilization effect on rice (a) and maize (b). Since we assume geoengineering starting in 2020 (year 1), year 36 is actually 2055. All lines are the average of crop production simulated by 10 climate models. The error bars on each line are one standard deviation of the 10 climate models including 30 climate conditions for each year. The horizontal gray lines are crop production of the control runs and the gray areas are crop natural variability. The vertical gray lines indicate the end of G2 geoengineering. The CO_2 fertilization effect can be estimated from the difference between the blue and the black lines.

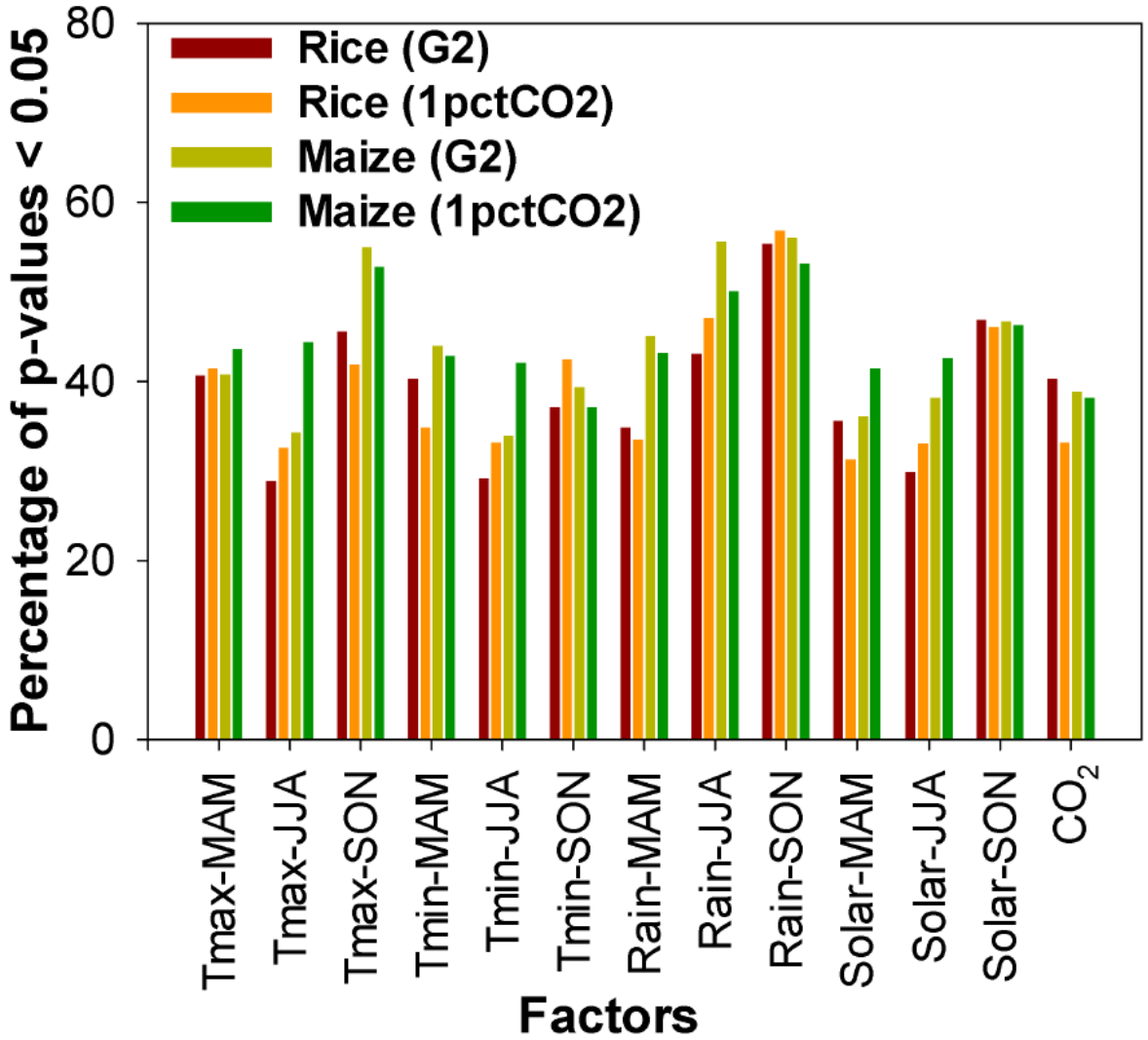

Figure 9. Percentage of *p*-values < 0.05 of 13 climate factors considered in linear regression. There are 10 (models) × 25 (locations) equations for each crop under each scenario. The regression uses 900 years of seasonal climate factors and crop yields.